

# A New Approach for Simulating Galaxy Cluster Properties

Y. Arieli<sup>1,2</sup>, Y. Rephaeli<sup>1,2</sup> & M. L. Norman<sup>2</sup>

<sup>1</sup> *School of Physics and Astronomy, Tel Aviv University, Tel Aviv, 69978, Israel*

<sup>2</sup> *Center for Astrophysics and Space Sciences, University of California, San Diego, La Jolla, CA 92093-0424*

## ABSTRACT

We describe a subgrid model for including galaxies into hydrodynamical cosmological simulations of galaxy cluster evolution. Each galaxy construct— or *galcon*— is modeled as a physically extended object within which star formation, galactic winds, and ram pressure stripping of gas are modeled analytically. Galcons are initialized at high redshift ( $z \sim 3$ ) after galaxy dark matter halos have formed but before the cluster has virialized. Each galcon moves self-consistently within the evolving cluster potential and injects mass, metals, and energy into intracluster (IC) gas through a well-resolved spherical interface layer. We have implemented galcons into the *Enzo* adaptive mesh refinement code and carried out a simulation of cluster formation in a  $\Lambda$ CDM universe. With our approach, we are able to economically follow the impact of a large number of galaxies on IC gas. We compare the results of the galcon simulation with a second, more standard simulation where star formation and feedback are treated using a popular heuristic prescription. One advantage of the galcon approach is explicit control over the star formation history of cluster galaxies. Using a galactic SFR derived from the cosmic star formation density, we find the galcon simulation produces a lower stellar fraction, a larger gas core radius, a more isothermal temperature profile, and a flatter metallicity gradient than the standard simulation, in better agreement with observations.

*Subject headings:* galaxies: clusters: general – methods: numerical

## 1. Introduction

Current hydrodynamic cosmological simulations of galaxy clusters show an appreciable level of inconsistency with results from high-precision optical and X-ray observations.

Discrepancies are particularly apparent in intracluster (IC) gas properties (e.g., Tornatore et al. 2003, Kay et al. 2007, Tornatore et al. 2007; for a recent review, see Borgani et al. 2008) - spatial distributions of density, temperature, and metallicity, but also in the stellar component for which simulations usually over-predict the stellar mass fraction while underpredicting the total number of galaxies (Nagamine et al. 2004 and references therein.). Physical processes, such as galactic winds, ram-pressure stripping, mergers of subclusters, energetic particle heating, and gravitational drag, affect the dynamical and thermal state of IC gas. Several attempts to implement some of these phenomena have been made (e.g., Kapferer et al. 2006, Domainko et al. 2006, Bruggen & Ruszkowski 2005, Sijacki & Springel 2006, Cora 2006, Kapferer et al. 2007), with some success in reconstructing IC gas properties. However, different combinations of these processes and their specific implementation in numerical codes generally result in quite different gas properties.

Because modeling star formation (SF) self-consistently requires prohibitively high level of spatial resolution, most current simulations use a SF prescription that follows the formation of collisionless star ‘particles’ which feedback mass and energy to IC gas (Cen & Ostriker 1992; Nagai & Kravtsov 2005). This approach overestimates the SF rate (SFR) at low  $z$  (Nagamine et al. 2004), which leads to a higher than expected star to gas mass ratio. In addition, feedback from the star particles is unresolved, leading to unrealistically low levels of gas (including metals) and energy transfer from galaxies into IC gas, and consequently insufficient suppression of cooling and gas overdensity in cluster cores. This unsatisfactory state motivates our attempt to develop a new method that partly overcomes current numerical limitations.

In this *Letter* we briefly describe a new approach (Section 2) for including galaxies in hydrodynamical cosmological simulations of cluster evolution which provides improved control over the relevant physical processes. Galaxies which are otherwise under-resolved (or absent!) are replaced with a physically-extended galaxy subgrid model which we refer to as a *galcon* within which SF, galactic winds, and ram pressure stripping of gas are modeled analytically. Galcons are initialized at high redshift after galaxy dark matter (DM) halos have formed but before the cluster has virialized. Mass, metals, and energy are injected from galcons into IC gas. In Section 3 we compare the results of our galcon simulation with a standard simulation using a popular star formation and feedback recipe, and summarize our main conclusions in Section 4.

## 2. Simulation and Modeling Procedures

Cluster evolution is followed using Enzo, a powerful adaptive mesh refinement (AMR) cosmological hydrodynamical code (Bryan & Norman 1997). A high resolution cosmological simulation with baryons is performed starting at an initial redshift  $z_i \simeq 60$ ; the evolution is stopped at  $z_r = 3 - 5$  (the 'replacement' redshift), where we know from observations the SFR peaked and early galaxies were already highly developed. At this time galactic halos with total mass  $10^9 - 10^{12} M_\odot$  within the Lagrangian volume of the cluster are identified by a halo finding technique. Since the dynamics of DM halos is followed, they are allowed to merge, but galcons in merged halos are still identified as separate systems. Also, no new galcons are created at  $z < 3$ , but this hardly matters since high-mass galaxies already formed by  $z \sim 3$ . and the baryon density profiles are fit by  $\beta$  models. Galcons with these analytic density profiles are inserted into the centers of each halo, and assigned the halo velocity. Each galcon's central density and outer radius are determined from the fit and the baryonic mass within the halo virial radius. An equal amount of baryons is removed from the simulated density field. Note that the total mass density field, which is the sum of DM, baryonic gas, and stars is not affected by this replacement. Thus, an unphysical instantaneous change in the simulated density distribution does not occur.

Both stellar and gaseous components are included in galcons, and since stars form in the same high gas density interstellar (IS) central regions that contain most of the gas and can be assumed to have initially roughly similar spatial distributions, it is reasonable to approximate both by the same  $\beta$ -profile parameters, but with different central densities. The mean initial baryonic mass density in galaxies can be determined by multiplying the mass density of halos from the Press & Schechter (PS, 1974) mass function by the universal baryonic density parameter  $\Omega_b$ . The stellar mass density is calculated by integrating the cosmic SFR density (to be specified below) over the interval  $[z_i, z_r]$ .

Having initialized galcons, we follow their motion dynamically using Enzo's N-body machinery and follow the mass and energy ejection processes that enrich and heat up IC gas - galactic winds and ram pressure stripping - through simple analytic models. Galactic winds reduce the total stellar mass while ram pressure stripping continuously reduces the galcon outer gas radius (as quantified below). Since galactic winds are SN driven, their elemental abundances are higher than in IS gas by a factor of  $\sim 3$ . We follow the enrichment by both processes, separately and jointly.

Observations of galactic winds (*e.g.*, Heckman 2003) provide direct evidence for the relation between the mass and energy ejection rates and the SFR,  $\dot{M}_*$ ,

$$\dot{E}_w = e_w \dot{M}_* c^2$$

$$\dot{M}_w = \beta_w \dot{M}_* , \quad (1)$$

where the parameters  $e_w$  and  $\beta_w$  are energy and mass ejection efficiencies, respectively, and  $c$  is the speed of light. The ejection efficiencies cannot be directly predicted from simple considerations, but they can be roughly estimated from observations (e.g., Pettini et al 2001; Heckman et al. 2001), from which typical values of  $e_w = 5 \times 10^{-6}$  and  $\beta_w = 0.25$  are adopted (e.g., Cen & Ostriker 1993, Leitherer et al. 1992).

An advantage of the galcon approach is analytic control over the SF history of each galaxy which we take from observations. The galactic SF history is determined indirectly from the closely related stellar mass density, which can be estimated by fitting multiband photometric observations to simulated galaxy spectra generated by a population synthesis model (e.g., Brinchmann & Ellis 2000, Cohen 2002, Glazebrook et al. 2004). Ideally, we would use the SF history of observed cluster galaxies for our galcons. As this information is not yet available to us, we instead use the observed cosmic SF density to illustrate our method. It has been suggested (Nagamine et al. 2006) that the cosmic SF density can be expressed as the sum of two exponential terms based on the characteristic SF times of disk and spheroid galaxies, where the scaling between the two components is determined by the spheroid to disk stellar mass ratio. The mean SFR in a galaxy can then be roughly estimated from the universal SFR rate by simply taking the ratio of the mass density of galaxies - determined from the PS mass function - to the observationally deduced universal SFR per unit volume. The two-parameter fit  $s(t) = 1.58 \times 10^{-2} t^\alpha \exp(-\gamma t) \text{ Gyr}^{-1}$ , with (cosmological time)  $t$  in Gyr,  $\alpha = -0.70$ , and  $\gamma = 0.07$ , represents well the SFR density. The total SFR in a galaxy at a given time, which is used to set the energy and mass ejection by galactic winds, can then be calculated by multiplying the above SFR density by the total mass of the galaxy.

SN ejecta from the galactic disk quickly interact through shocks and mix with the surrounding IS gas. Thus, the wind contains a blend of metals from stars and IS medium. However, the fraction of gas in the ejecta cannot accurately be determined. We assume that most of the wind ejecta come from the stellar component whose metallicity is approximately solar; accordingly, we subtract the energy and mass carried by the wind from the galcon stellar content, and increase the metallicity of IC gas by an amount which is proportional to galcon mass ejecta. The transfer of mass and energy to IC gas is implemented by isotropically distributing the ejecta over a thin shell - typically a few kpc - surrounding the outer galcon radius. Also, since the level of SN activity is roughly linearly proportional to the local star density, the wind does not modify the spatial stellar profile. Thus, we only adjust the central density of the stellar component to reflect the loss of stellar material.

Ram pressure stripping is implemented by determining (at any given time) the stripping

radius, where the local IC gas pressure is equal to the local galactic IS pressure, simply assuming that all IS gas outside this radius is stripped on a relatively short dynamical timescale. We generalize the analytic Gunn & Gott (1972) stripping condition by including the (generally dominant) contribution of DM to the galactic gravitational force (which was ignored in some previous works). Observational evidence supports the expectation that stripping truncates the gaseous disk but does not modify the gas profile; neither does it appreciably affect the dynamics of the stellar and DM components of the galaxy (Kenney & Koopmann 1999; Kenney, Van Gorkom & Vollmer 2004). Thus, the outer radius of the galcon gas component is reduced to the stripping radius without modifying the central density or the scale radius of its profile.

### 3. Results

In order to quantify the improvements in the description of the evolution of IC gas in our new code, we have performed two high resolution runs with AMR and radiative cooling (Sutherland & Dopita 1993). The first - hereafter the galcon run (GR) - included the additional physical processes and galcons, whereas the second - the comparison run (CR) - included the SF and feedback recipe of Cen & Ostriker (1992). The setup of both runs includes a root grid of  $128^3$  cells which covers a comoving volume of  $54 \text{ Mpc}^3$  with two nested inner grids. The most refined grid covers a comoving volume of  $27 \text{ Mpc}^3$  divided into  $128^3$  cells and can be further refined by up to 5 levels, with a maximum  $\sim 9 \text{ kpc}$  resolution.

Both runs were initialized at  $z = 60$  assuming a  $\Lambda$ CDM model with  $\Omega_m = 0.27$ ,  $\Omega_\Lambda = 0.73$ ,  $\sigma_8 = 0.9$ , and  $h = 0.71$  ( $H_0$  in units of  $100 \text{ km s}^{-1} \text{ Mpc}^{-1}$ ). The CR was evolved continuously to  $z = 0$ . The GR was stopped at  $z = 3$ , and a halo-finding algorithm (Eisenstein & Hut 1998) was used to locate 89 galactic halos with mass in the range  $10^9 - 10^{12} M_\odot$  within a volume which eventually collapsed to form the cluster. The baryonic content of these halos was analyzed and replaced by galcons, as described in section 2. The simulation was then evolved to  $z = 0$  with the additional physical processes and galcons. Both simulations included radiative cooling over the entire ( $z \geq 0$ ) evolution. A fuller description of the simulation and the models will be given in a forthcoming paper (Arieli, Rephaeli & Norman, in preparation).

Relatively rich  $\sim 5.4 \times 10^{14} M_\odot$  clusters with similar global properties were generated in both runs. Near equality in the global properties of the simulated clusters is expected since (identically treated) DM dynamics govern cluster formation and evolution. However, the composition of the cluster and the properties of the baryonic component, particularly in the core, are substantially different. A significant difference is seen in the number of cluster

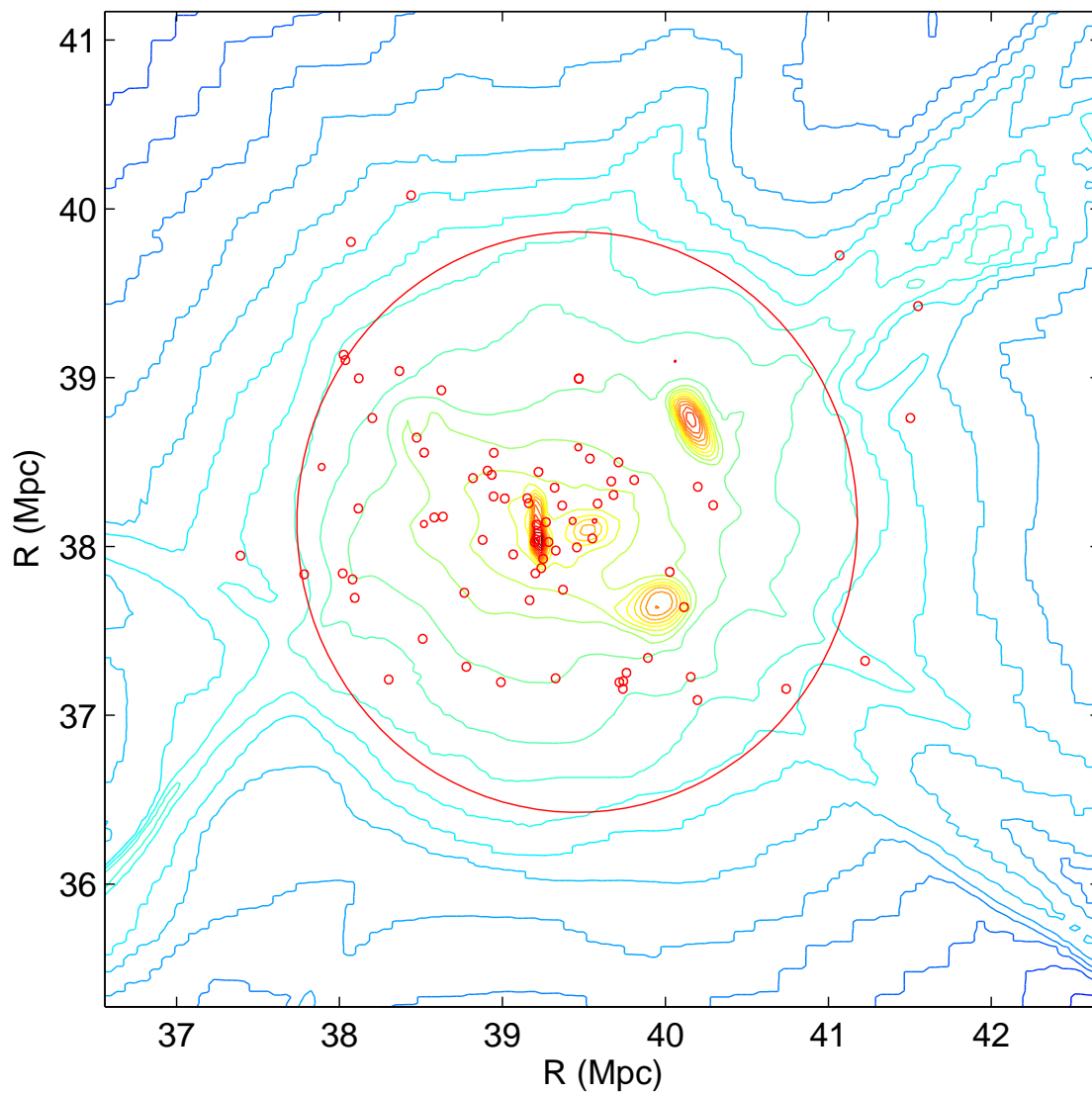


Fig. 1.— Positions of galaxies at  $z=0$  are shown over a map of projected gas density iso-density contours. The red circle indicates the virial radius,  $R_v = 1.71 \text{ Mpc}$ .

galaxies; we identified a final number of 81 galaxies within the virial radius of the GR cluster (Fig. 1), whereas only 6 galaxies were identified in the CR cluster. Thus, The drastically lower number of identified galaxies in the CR cluster stems from inadequate force resolution which results in the unphysical merging of galaxy DM halos (the “overmerging problem”; Moore et al. 1996, Klypin et al. 1999.) Klypin et al. 1999 argue that a *proper* force resolution of  $\leq 2h^{-1}$  kpc and mass resolution  $\leq 10^9 h^{-1} M_{\odot}$  is required for galaxy mass halos to survive in the dense cluster core. While our Enzo simulation meets the mass resolution requirement, its *comoving* force resolution is  $7.8 h^{-1}$  kpc – less than required. However, by replacing the baryon content of galaxies with galcons at  $z=3$ , where the proper force resolution is four times better, we “lock in” their mass distribution in a resolution-independent way. During the N-body dynamics phase of the calculation, the galcon’s extended mass distribution is deposited to the mesh where it helps anchor the DM halo despite less than optimal force resolution.

Our galaxies remain intact as they pass through the cluster core as they are “indestructible.” This has important consequences for IC gas properties, as we discuss next.

### 3.1. Star formation and heating

SF history is a central driver of gas feedback processes. It is therefore very important to verify that our GR simulation produces the required heating to overcome overcooling, and results in a reasonable stellar mass fraction. As stated before, the simulation does not directly input the observational cosmic SFR to each galaxy. Rather, it only incorporates the functional behavior of the SFR, with its actual level and history determined based on the galcon mass and redshift. The SFR density in the GR and CR clusters is shown in the top left panel of Fig. 2. The cosmic SFR density in the GR cluster is consistent with observations; the agreement is good at high  $z$ , whereas below  $z \sim 0.5$  the SFR density is at the lower end of the observationally deduced range. This could possibly be due to the lack of galcon mergers, events during which the SFR is enhanced. Analysis of the simulation does show that at  $z = 0$  a small number of galcons are sufficiently close to merge. However, mergers and the associated boost of SF are not implemented in the current version of the simulation; their impact will be explored in planned subsequent work. The star to gas mass ratio is  $\sim 9.5\%$ , in good agreement with the observationally deduced value (e.g., Balogh et al. 2001, Wu & Xue 2002).

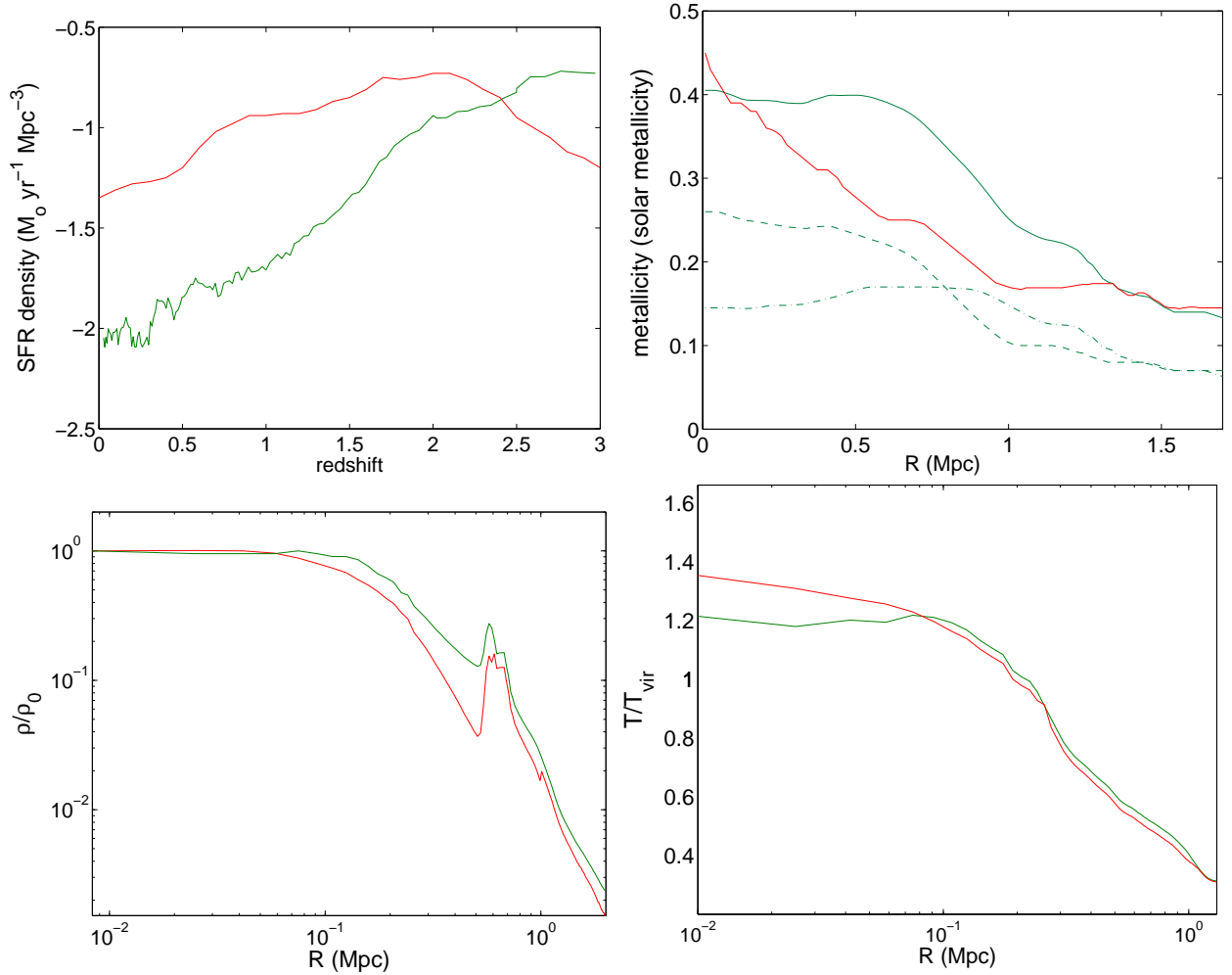


Fig. 2.— The SFR density (top left) and the profiles of IC gas metallicity (top right), density (bottom left), and temperature (bottom right) in the simulated GR (green) and CR (red) clusters are shown in the four panels. Also shown are the separate contributions to the metallicity from wind ejecta (dashed-dotted line) and from ram pressure stripping (dashed line) in the GR cluster.



### 3.2. Gas metallicity, density and temperature

Metallicity in the GR cluster (top right panel of Fig. 2) is due to enrichment by both winds and ram pressure stripping, with the former process being more effective at higher redshifts, since it is driven by shocks from SN that are then more prevalent. At these early periods of cluster evolution a higher fraction of galaxies are outside the cluster core, where metals are preferentially deposited. As the cluster evolves galaxies are more centrally distributed, so metals are more effectively spread in the central region. This results in an approximately constant metallicity across the cluster. On the other hand, because gas stripping depends on the local IC gas density, which builds up as the cluster evolves, the contribution to the metallicity is larger at lower  $z$ , and is more concentrated in the high density core, resulting in a substantial metallicity gradient.

The total metallicity in the GR cluster is roughly constant out to  $\sim 700$  kpc; it decreases at larger radii. Its mean value across the cluster is  $0.32Z_{\odot}$ , within the observationally determined range,  $(0.3-0.4)Z_{\odot}$ . The mean metallicity in the CR cluster is  $0.25Z_{\odot}$ , somewhat lower than typical. Moreover, its steep decline already in the central region is also at odds with observations, which show a nearly constant metallicity in the central few hundred kpc (Hayakawa et al. 2006, Pratt et al. 2006), with the exception of a small galactic-size region at the cluster center where the metallicity is higher (Snowden et al. 2008). A much shallower gradient is observed in cooling flow clusters (e.g., De Grandi et al. 2004), but our simulated clusters have no cooling flows. We conclude that in our GR simulation - which includes galactic winds and ram pressure stripping - both the level of metallicity and its spatial profile are consistent with observations, whereas neither property is well reproduced in the CR cluster.

The density profiles (bottom left panel of Fig. 2) are similar at large radii, including a steep hump at  $r \sim 600$  kpc, indicating the location of a very massive clump. The profiles flatten towards the center, but the GR cluster has a substantially larger core of  $\sim 180$  kpc compared to a relatively small core of 50 kpc in the CR cluster. The shape of the density profile in the central region is mainly determined by the fraction of IC gas that cooled down and converted into stars. The absence of sufficient feedback in the CR cluster results in too much cool gas in the inner core. Excessive cooling results in a small core as well as an unrealistically high number of stars, while the GR cluster includes stronger and more efficiently spread feedback, resulting in suppression of overcooling and in a larger core.

In a non cooling-flow cluster the core is isothermal and the temperature profile declines rapidly with radius outside the core (e.g., De Grandi & Molendi 2002). This decrease is indeed seen in both clusters at radii larger than  $\sim 200$  kpc (bottom right panel of Fig. 2). However, only the GR cluster has a flat isothermal core, while in the CR cluster the

temperature continues a moderate rise towards the center. In the CR simulation a local SF prescription is used; this leads to formation of star groups which are at locations where the gas is dense and cold. Feedback heating from these star groups remains localized to their immediate inner core region, too concentrated to heat the outer core. This is particularly apparent at lower  $z$ . In contrast, in our GR simulation the implementation of winds out of galcons effectively spreads out the heating over a much larger volume, resulting in a large isothermal core.

#### 4. Conclusion

The combination of our galaxy constructs and new semi-analytic modeling of the relevant physical processes yields a powerful tool that is capable of reproducing the basic properties of clusters. Our new approach successfully describes SF and the basic properties of IC gas, including its metallicity and energy feedback. The ever improving observational data motivate further development of the code and inclusion of additional physical processes previously unaccounted for, such as AGN feedback. We plan to improve the description of galactic mergers, and intend to implement an improved algorithm for replacing galactic halos with new galcons as the cluster evolves, instead of performing this replacement only at an initial redshift as has been done in the simulations reported here. Ongoing work on this project will hopefully lead to a much better understanding of the intrinsic properties of both DM and baryons in clusters.

We thank Drs. Alexei Kritsuk and Brian O’Shea for many useful discussions, and the referee for useful comments. Work at Tel Aviv University was supported by ISF grant 225/03.

#### REFERENCES

- Balogh M.L. et al. 2001, *MNRAS* 326, 1228.
- Borgani S. et al. 2003, *astro-ph/0310794*.
- Borgani S. et al. 2008, *SSRv* 134, 269.
- Borgani S. et al. 2008, *SSRv* 134, 379.
- Brinchmann J. & Ellis R. 2000, *ApJ*. 536, L77.

- Bruggen M. & Ruszkowski M. 2005, *astro-ph/0512148*.
- Bryan G. L. & Norman M. L. 1997, in ASP Conf. Ser. 123, Computational Astrophysics, ed. D. A. Clarke & M. Fall (San Francisco: ASP), 363.
- Cora S.A. 2006, *MNRAS* 368, 1540.
- Cen R. & Ostriker J.P. 1992, *Ap. J. Lett.* 399, L113.
- Cen R. & Ostriker J.P. 1993, *ApJ.* 417, 404.
- Cohen J. G. 2002, *ApJ.* 567, 672.
- De Grandi S. et al. 2004, *Astron. Astrophys.* , 419, 7.
- De Grandi S. & Molendi S., 2002, *ApJ.* 567, 163.
- Domainko, W., et al. 2006, *Astron. Astrophys.* 452, 795.
- Eisenstein D. J. & Hut P. 1998, *ApJ.* 498, 137.
- Glazebrook K. et al. 2004, *astro-ph/0401037*.
- Gunn J.E. & Gott J.R. 1972, *ApJ.* 176, 1.
- Hayakawa A. et al. 2006, *Publ. Astron. Soc. Japan* 58, 695.
- Heckman, T. M. et al. 2001, *ApJ.* 558 56.
- Heckman, T. M. 2003, *RevMexAA (Serie de Conferencias)* 17, 47.
- Kapferer W. et al. 2006, *Astron. Astrophys.* 447, 827
- Kapferer W. et al. 2007, *Astron. Astrophys.* 466, 813.
- Kay et al. 2007,
- Kenney J.D.P. & Koopmann R. 1999, *Astron. J.* 117, 181.
- Kenney J.D.P., Van Gorkom J. H. & Vollmer B. 2004, *Astron. J.* 127, 3361.
- Klypin A., Gottlober S. & Kravtsov A.V. 1999, *ApJ.* 516, 530.
- Leitherer C., Robert C. & Drissen L. 1992, *ApJ.* 401, 596.
- Moore B., Katz N. & Lake G. 1996, *ApJ.* 457, 455.

- Nagai D. & Kravtsov A.V. 2005, *ApJ.* , 618, 557
- Nagamine K. et al. 2004, *ApJ.* 610, 45.
- Nagamine et al. 2006, *ApJ.* 653, 881.
- Pettini et al. 2001, *ApJ.* 554, 981.
- Pratt G.M. et al. 2006, *astro-ph/0609480*.
- Press, W. H., & Schechter, 1974, *ApJ.* 187, 425
- Sijacki D. & Springel V. 2006, *MNRAS* 366, 397.
- Snowden S.L. et al. 2008, *Astron. Astrophys.* 478, 615.
- Sutherland R.S. & Dopita M.A. 1993, *Ap. J. Supp.* 88, 253.
- Tornatore L. et al. 2003, *astro-ph/0302575*.
- Tornatore L. et al. 2008,
- Wu X.P. & Xue Y.J. 2002, *ApJ.* 569, 112.